Independent Passive Mechanical Behavior of Bovine Extraocular Muscle Compartments

Andrew Shin,[1,2] *Lawrence Yoo,*[1] *Zia Chaudhuri,*[1] *and Joseph L. Demer*[1,3–5]

Purpose. Intramuscular innervation of horizontal rectus extraocular muscles (EOMs) is segregated into superior and inferior (transverse) compartments, while all EOMs are also divided into global (GL) and orbital (OL) layers with scleral and pulley insertions, respectively. We sought evidence of potential independent action by examining passive mechanical coupling between EOM compartments.

Methods. Putative compartments of each of the six whole bovine anatomical EOMs were separately clamped to a physiologically controlled, dual channel microtensile load cell (5-mN force resolution) driven by independent, high-speed, linear motors having 20-nm position resolution. One channel at a time was extended or retracted by 3 to 5 mm, with the other channel stationary. Fiducials distributed on the EOM global surface enabled optical tracking of local deformation. Loading rates of 5 to 100 mm/sec were applied to explore speeds from slow vergence to saccades. Control loadings employed transversely loaded EOM and isotropic latex.

Results. All EOM bellies and tendons exhibited substantial compartmental independence when loaded in the physiologic direction, both between OL and GL, and for arbitrary transverse parsings of EOM width ranging from 60%:40% to 80%:20%. Intercompartmental force coupling in the physiologic direction was less than or equal to 10% in all six EOMS even for saccadic loading rates. Coupling was much higher for nonphysiologic transverse EOM loading and isotropic latex. Optical tracking demonstrated independent strain distribution between EOM compartments.

Conclusions. Substantial mechanical independence exists among physiologically loaded fiber bundles in bovine EOMs and tendons, providing biomechanical support for the proposal that differential compartmental function in horizontal rectus EOMs contributes to novel torsional and vertical actions. (*Invest Ophthalmol Vis Sci.* 2012;53:8414–8423) DOI: 10.1167/iovs.12-10318

From the [1]Department of Ophthalmology, Jules Stein Eye Institute, Los Angeles, California; the Departments of [2]Mechanical Engineering, [3]Biomedical Engineering Interdepartmental Program, [4]Neuroscience Interdepartmental Program, and [5]Neurology, University of California, Los Angeles, Los Angeles, California.

Supported by grants from the National Eye Institute (EY08313 and EY0331), the Shaw Family Endowment Fund, Research to Prevent Blindness, and the Leonard Apt Professor of Ophthalmology (JLD).

Submitted for publication June 1, 2012; revised October 1 and November 18, 2012; accepted November 19, 2012.

Disclosure: **A. Shin**, None; **L. Yoo**, None; **Z. Chaudhuri**, None; **J.L. Demer**, None

Corresponding author: Joseph L. Demer, Jules Stein Eye Institute, 100 Stein Plaza, UCLA, Los Angeles, CA 90095-7002; jld@ucla.edu.

Skeletal muscles often have multiple neuromuscular compartments that are controlled by independent motor neuron pools.[1–3] Examples include transversus abdominis,[3] cricothyroid,[4] and triceps brachii[5] that are independently innervated by separate nerve branches. It has been suggested that extraocular muscle (EOM) has more motor units than apparently required by known ocular motility mechanisms.[6,7] Peng et al.[8] traced the intramuscular arborization of the abducens nerve within the lateral rectus (LR) EOMs of monkeys and humans, and observed that the nerve bifurcated into non-overlapping superior and inferior territories that remained segregated throughout the EOM's length. Costa et al.[9] subsequently confirmed Peng's[8] report of compartmentalized LR innervation, and extended the study by tridimensional reconstruction of nerve arborizations to the inferior (IR), medial (MR), and superior rectus (SR) EOMs of humans and monkeys. The consistent finding was that the LR and MR motor nerves were divided into two divisions, superior and inferior, with approximately equal size, corresponding to similarly proportioned compartments of EOM fibers. In contrast, the IR and SR EOM motor nerves were highly mixed throughout each EOM, inconsistent with compartmental specialization. On this basis, Costa et al.[9] suggested that differential innervation in horizontal rectus EOM compartments can potentially mediate previously unrecognized vertical oculorotary actions for these EOMs. While Costa et al.[9] did not suggest that the dual compartments of the horizontal rectus EOMs are always differentially activated, these authors proposed that differential innervation might occur under some physiologic conditions. Recently, functional evidence for differential compartmental activation of the human LR was obtained from magnetic resonance imaging (MRI) during ocular counter-rolling induced by head tilt.[10]

In addition to the superior and inferior neuromuscular compartments in the horizontal rectus EOMs, an orthogonal compartmentalization of all six anatomical EOMs has long been recognized, distinguishing the global (GL) and orbital layers (OL). According to the active pulley hypothesis (APH), the OLs insert in connective tissue rings, called pulleys, which pass through the global layer fibers that in turn insert on the sclera to rotate the eye. During EOM contraction, the pulleys shift posteriorly so as to cause EOM pulling directions to shift by half the change in ocular orientation, producing a mechanical implementation of Listing's Law of ocular torsion, and effectively rendering the sequence of ocular rotations commutative for distant targets with the head upright and stationary.[11–15] The APH postulated at least some degree of mechanical independence of fibers in the OL versus GL, since each layer is postulated to be independently controlled to maintain Listing's Law.

There is no anatomical basis for predicting the degree of mechanical independence of groups of EOM fibers. Skeletal muscles are considered to encompass four morphologies of fiber orientation: parallel, convergent, pennate, and sphincter.[16] Although EOMs differ in many respects from skeletal

Investigative Ophthalmology & Visual Science, December 2012, Vol. 53, No. 13

muscles, their fiber organization is generally regarded to have a roughly parallel arrangement that might be supposed to have some independence among fibers. Various claims have been made about the anatomical degree to which EOM fibers are mutually coupled longitudinally and transversely. Observations based upon serial transverse sections of undisturbed, whole human and monkey orbits suggest that rectus EOM fibers are arranged in roughly parallel bundles.[17,18] Mayr et al.[19] studied teased fiber preparations of cat EOMs, and reported that while all OL fibers run from tendon to tendon, in the GL only the multiply-innervated fibers (MIFs) do so, while the singly-innervated fibers (SIFs) are usually arranged in series of two or three fibers interconnected by myomyous junctions with frequent fiber splitting. Mayr et al.[19] also observed end-to-side connections between SIFs and MIFs. In the approximately 22-mm long isolated superior rectus (SR) OL of a juvenile rabbit, Davidowitz et al.[20] traced 94 fibers in four fascicles of the and found the SIFs to extend 5 to 8 mm in length, and MIFs to extend 10 to 19 mm in length. Davidowitz et al. observed several instances fiber splitting in MIFs.[20] Based upon myosin expression in rabbit EOM, McLoon et al. proposed a complex variety of fiber morphologies, with some extending the entire EOM length, and other shorter fibers in series arrangement.[21] Harrison et al., reported that individual EOM fibers of rabbit and monkey are shorter than the overall EOM, and in rabbit SR change their relationships with adjacent fibers along their longitudinal course.[22] Regardless of the arrangement of EOM fibers, and regardless of the presence of connective tissue within EOMs, anatomical studies cannot be decisive regarding the overall mechanical behavior of EOM subgroups considered on a larger scale. This issue can only be resolved by direct biomechanical measurements of EOM compartments that have not heretofore been available.

Materials engineering provides several approaches to characterize internal mechanical coupling. Coupling between normal and shear directional stresses or strains describes some of the moduli of anisotropic materials. The shear coupling ratio is defined as the ratio of the shear strain to normal strain associated with the axis of the normal strain.[23–25] Tensile or shear loading tests are performed to determine the shear coupling ratio of materials such as wood[26] or composites of graphite filaments embedded in epoxy resins.[27] Adhesive force measurement between composites could be considered similar to the coupling between EOM compartments, in terms of local force generation between two layers. Microbond techniques,[28–30] single-fiber fragmentation,[31–33] and microindentation/microdebonding techniques[34–36] have been employed for measuring fiber-matrix adhesion in composite materials. To date, none of these techniques have been employed to investigate the compartmental mechanical behavior of EOM.

Motivated by anatomical findings for suggesting compartmentalized intramuscular innervation of horizontal rectus EOMs, and OL/GL compartmentalization in all EOMs, this study aimed to investigate the potential for independent passive mechanical behavior of EOM compartments in large and easily available bovine specimens. While passive loading does not replicate the process of active tension generation in an EOM, it should reflect force distribution among fibers, and probably reflects behavior during passive physiologic elongation by the EOM's antagonist. A finding of substantial mechanical coupling between EOM compartments during passive elongation would decisively exclude the Costa et al.[9] hypothesis of physiologically independent action of horizontal rectus EOM compartments, and would challenge the proposition of the APH that the OL is innervated differently from the GL in each of the anatomical EOMs. Conversely, a finding of substantial mechanical independence between compartments would allow the foregoing hypotheses to remain under consideration.

Methods

Dual Channel Microtensile Testing

A custom dual channel microtensile load cell was constructed, consisting of two horizontally mounted, tensile loading devices capable of acting with less than 1-mm lateral spacing. In order to maintain high mechanical stiffness, all components were mounted, using heavy aluminum or steel hardware, to a 12.5-mm thick aluminum optical bench foundation plate. It was verified that the structure did not deform measurably during tissue loading, so that measurements reflected tissue properties without influence of instrument compliance. Each mechanical channel could be pulled independently while force was recorded independently in the corresponding channel. In each channel, a servo-controlled electromagnetic linear motor (Ibex Engineering, Newbury Park, CA) capable of high speed (controllable to a maximum of 100 mm/sec) and fine resolution (20 nm) was mounted in line with an S-shaped semiconductor strain gauge (FUTEK Advanced Sensor Technology, Irvine, CA) having 5 mN resolution. This servomotor permits precise, independent control of both linear position and linear speed. Each strain gauge was, in turn, attached to a 127-mm long stainless steel tensile shaft that passed into a closed physiologic chamber through a frictionless air bearing that served as its mechanical support. Inside the physiologic chamber the tensile shaft was attached to a high friction, serrated stainless steel compression clamp to engage one end of the specimen under test. The other specimen end was similarly clamped to a tensile shaft fixed to the opposite end of the load cell. When the linear motor elongated one of the channels via the tensile shaft, the strain gauge indicated the tensile force in the corresponding channel.

Specimens under test were enclosed in a physiologic chamber with transparent walls whose lower portion contained a water bath heated under feedback control to maintain 100% humidity and 37°C temperature in the overlying air adjacent the specimen, as measured by a thermocouple. A high resolution video camera with 50-mm macro lens (Canon EOS 5D Mark II; Canon U.S.A., Lake Success, NY) was mounted above the specimen outside the physiologic chamber. Since the air in the physiologic chamber was saturated with water vapor to prevent evaporation from the specimen under test, the upper surface of the chamber was coated with an anticondensation compound to inhibit fogging of the chamber wall during photography of the specimen. Figure 1 illustrates the schematic drawing and photograph of the dual channel load cell.

Specimen Preparation

Fresh heads of cows aged 20 to 30 months were obtained from a local abattoir (Manning Beef LLC, Pico Rivera, CA). In the laboratory, orbits were carefully dissected for extraction of EOM and connective tissue. Transport time from abattoir to laboratory was approximately 1 hour, and 2 hours additionally elapsed for dissection and preparation of EOMs for experiments. For most experiments, any opaque tissue sheaths were carefully dissected away from the EOMs using microsurgical instruments, so that surface fiducials could be optically imaged. In control experiments, the connective tissue sheathes of some specimens were left intact to ascertain possible effect of the sheaths. Representative photographs of excised bovine EOMs from our laboratory have been published elsewhere.[37]

Transverse Compartments

Multiple specimens of all six anatomical EOMs were extracted and prepared for transverse compartment experiments. Tendons and a small amount of terminal GL were sharply excised to assure that specimens included both OL and GL. Varying with bovine age, average

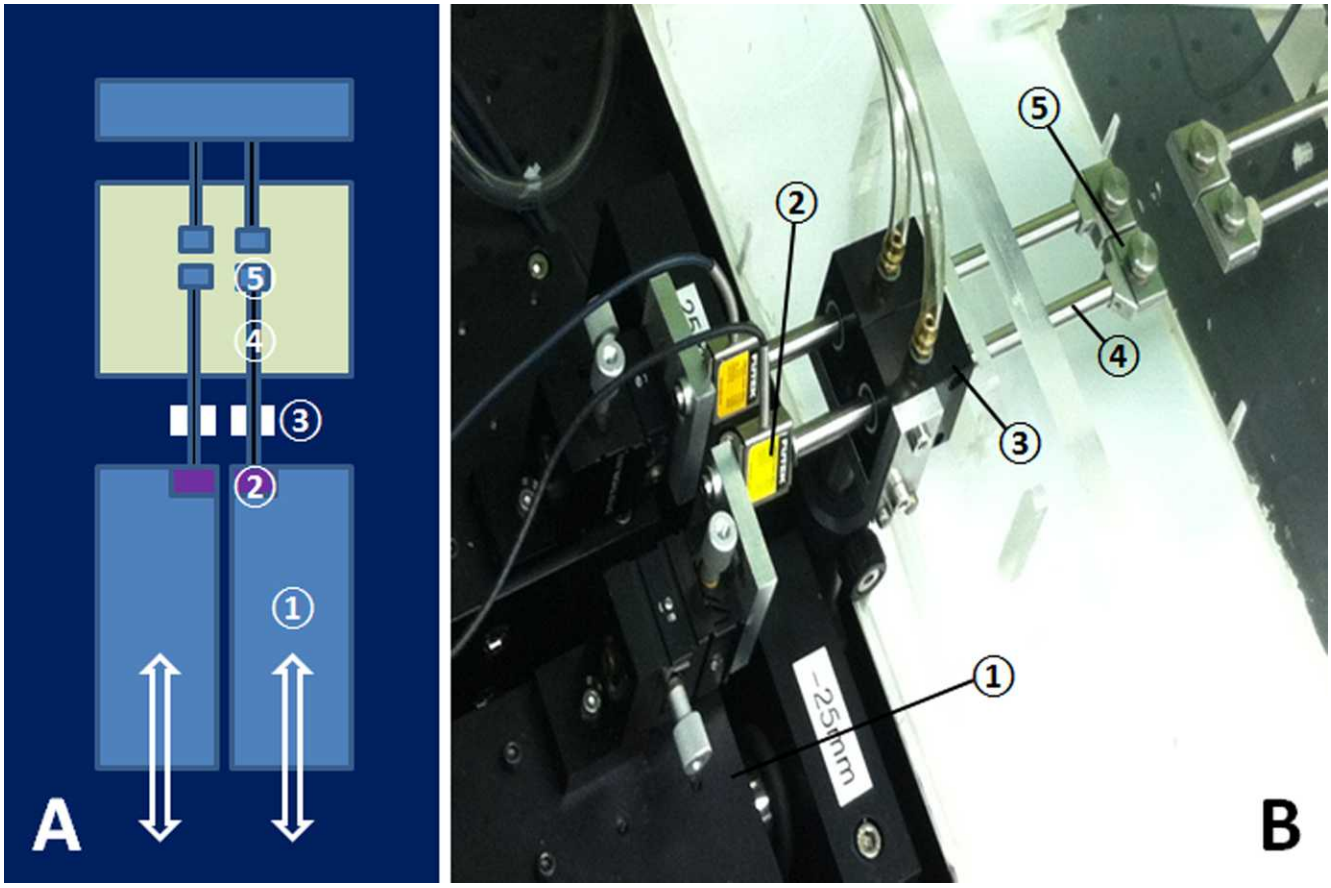

Figure 1. Dual channel microtensile load cell. (**A**) Schematic cartoon. Two linear motors moved independently, and generated tensile forces in each compartment of the tissue placed in the clamps. (**B**) Photograph of apparatus. In each adjacent channel, a linear motor (*1*) attached to a strain gauge (*2*) was coupled via a frictionless air bearing (*3*) through which passed a tensile shaft (*4*) connected to the specimen clamp (*5*).

specimen length after tendon removal was 45 ± 7 mm (SD). Depending upon the anatomical EOM, the ratio of length to greatest transverse width ranged from 2:1 to 5:1. Whole fresh EOM tissue is difficult to clamp uniformly because of its moisture and lack of intrinsic friction. It was critical to prohibit specimen slip relative to the clamp during experimental loading that would have introduced serious artifacts. For maximizing friction between the clamp and the specimen, a serrated clamp was fabricated of stainless steel using a computer-controlled mill. Prior to clamping, both broad surfaces of each specimen end were fixed using surgical suture and cyanoacrylate glue between 5-mm long layers of thin cardboard folded over the specimen's end to form an anchor that was placed in the clamp. Thus, the terminal 5 mm of each end of the specimen was contained within a clamp. The end of the specimen attached to moving clamps was sharply divided longitudinally (e.g., between superior and inferior portions for horizontal rectus EOMs) using a scalpel over a short distance of 1 to 3 mm into the EOM and clamped separately to the two load cell channels, while the fixed end was clamped to one broad clamp. This short longitudinal division at the elongating end was the minimum length necessary to prevent the elongating portion of the specimen from folding onto the fixed portion clamp, and creating a collision artifact. Figure 2 illustrates the arrangement for testing transverse compartmentalization of horizontal rectus EOMs.

GL/OL Compartments

All EOMs consist of GL and OL that have scleral and pulley insertions, respectively. Since the OL is located on the EOM's orbital surface and inserts on pulley connective tissue, special care was necessary to isolate the OL insertion. First, the pulley tissue for each EOM was identified, and carefully dissected free of external attachments. Then, the GL tendon was detached from the scleral insertion, and the tendon itself was sharply excised from the GL. Excess tissue in the distal part of the OL attachment was trimmed to the width of the GL. The GL, and the OL attachment, were then glued using cyanoacrylate between folded layers of thin cardboard to provide secure mechanical anchors held in the clamps (Fig. 3). Since both OL and GL extend over the full width of each EOM, a wider clamp was necessary for the GL/OL experiments than was required for transverse compartment experiments (Fig. 3). Other details for specimen mounting were the same as for the transverse compartment experiment. Figure 3 also illustrates specimen orientation for OL and GL experiments. Although the connective tissue contiguous with the OL insertion was expected to undergo some stretching during tensile testing, this effect does not alter the tension measured in the OL since the tissues are in mechanical series with the strain gauge.

Experimental Procedure

Preloading of approximately 20 gram force (gf) was applied to avoid slackness of specimens; ancillary experiments verified that the exact value of preload did not affect results appreciably. Only one channel at a time was extended in 3-mm increments for transverse compartment experiments, or 5 mm for GL/OL compartment experiments, while the other channel remained stationary during force recording in both channels. Because elongations were to fixed distances, resulting tensile forces reached an early peak and declined subsequently. Data were collected during the first 50 seconds of each elongation, although analysis was confined to the first 5 seconds. All six EOMs were tested at three different loading rates of 5, 20, and 100 mm/sec to investigate

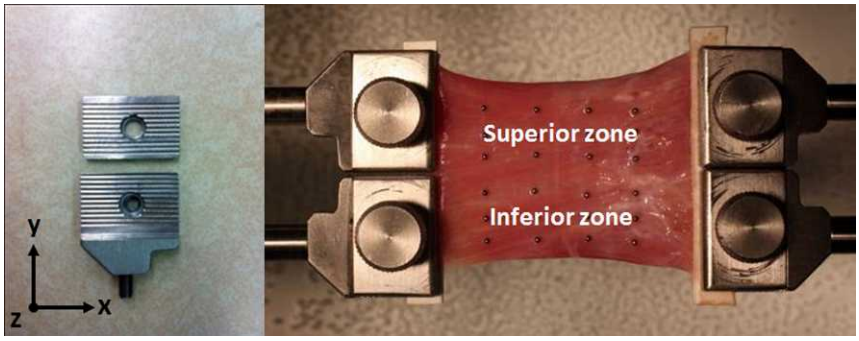

Figure 2. Transverse compartment testing configuration of medial rectus EOM. The specimen was aligned in the x-y plane. Metal bead fiducials are visible as an array of dots on the EOM global surface.

velocity dependence. During transverse compartment tests, fine reflective metal bead fiducials (1-mm diameter) were distributed in a regular array on the global surface for high definition video tracking to visualize local displacement throughout each EOM.

In addition to experiments in which tension was incrementally increased by specimen elongation, control experiments were performed in which tension was decreased by reducing elongation in one EOM compartment. In these experiments, each specimen was elongated to 9 mm to generate initial tension. After tension stabilized, one compartment was shortened 3 mm in the direction of compression (reduced tension) at 5 mm/sec, while the other compartment remained stationary. Data processing was same as for the original experiments, calculating the coupling fraction.

Coupling Fraction and Displacement Ratio

To investigate coupling between compartments, two parameters were defined: Coupling Fraction (CF) and Displacement Ratio (DR). CF is defined as the maximum force in the stationary compartment (F_s) divided by the maximum force in the moving compartment (F_m). A value of CF = 0 would imply that the two compartments are totally independent; a value of CF = 1 implies totally dependent coupling. In an analogous manner, DR is defined as the maximum local displacement of any individual fiduicial marker in the stationary compartment (D_s) divided by the maximum displacement of the spatially corresponding fiducial in the moving compartment (D_m).

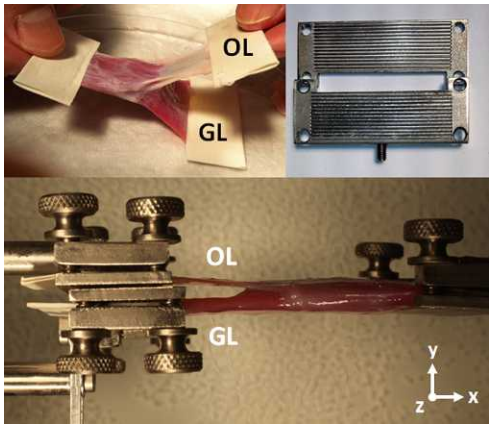

Figure 3. GL/OL compartment testing arrangement. A wider clamp was fabricated to span the entire tendon width. The specimen was aligned on the x-z plane. The abbreviations GL and OL indicate the points of force application that were coupled to these two layers; the cardboard marked OL was attached to connective tissue to which the OL fibers insert. The cardboard anchor on the OL's anchoring connective tissue was left long to avoid mechanical interference with the GL.

Results

Transverse Compartment Coupling

The degree of mechanical coupling between the transverse compartments of 15 EOM specimens was tested at 5, 20, and 100 mm/sec loading rates to fixed extensions not exceeding 5 mm. Representative specimen photographs and time series data are illustrated in Figure 4. In the time series data, positive values indicate tensile force, and negatives values indicate relative compressive force. Force coupling to the stationary channel reduces its tensile force, thus, appearing as relative compressive force. These experiments were performed for samples of all rectus and both oblique EOMs, all of which exhibited less than 10% CF under all testing conditions, and so reflecting a high degree of compartmental independence during tensile loading. For five specimens elongated to 3 mm at each loading rate, mean CF values for equal-sized compartments were 5.6 ± 0.3%, 4.9 ± 0.1%, and 4.1 ± 0.1%, respectively (Table 1). These findings indicate that CF varied inversely with loading rate, because of differences in the behavior of F_m and F_s. As loading rate increased, F_m increased (111.9, 133.1, and 142.4 gf, respectively), but numerator F_s remained almost constant (6.3, 6.5, and 5.8 gf, respectively), so their ratio decreased.

Local displacement information was also obtained from shifts of a rectilinear array with unloaded spacing of 6 mm between columns and 3 mm between rows of metal bead fiducials placed on the global surface of each EOM (Fig. 4). Locations of metal bead locations before and after tensile elongation were measured optically. Local displacements of each bead were computed as the two-dimensional differences between positions before and after elongation. Displacements of each fiducial distributed throughout the EOM were calculated for mapping the displacement field. Figure 5 illustrates an example displacement field obtained at the 5-mm/sec loading rate. Five specimens were tested and displacements were averaged in the x and y directions. The specimen at the fixed clamp necessarily has zero displacement, and the elongated end of the specimen at the moving clamp has the greatest displacement equal to that imposed by the load cell actuator. Therefore, displacement data in the first column near the moving clamps, which incorporates accumulated local displacements in the EOM, were used to determine average DR values in each compartment. Mean DR values were 5.4 ± 0.1%, 5.4 ± 0.1%, and 5.3 ± 0.1% at the three loading rates, respectively (Table 1). As may be seen from Table 1, DR was approximately 5%, independent of loading rate.

From displacement fields (Fig. 5), local displacement can be analyzed in two-dimensions of linear position for each fiducial before and after loading. In each compartment, all local

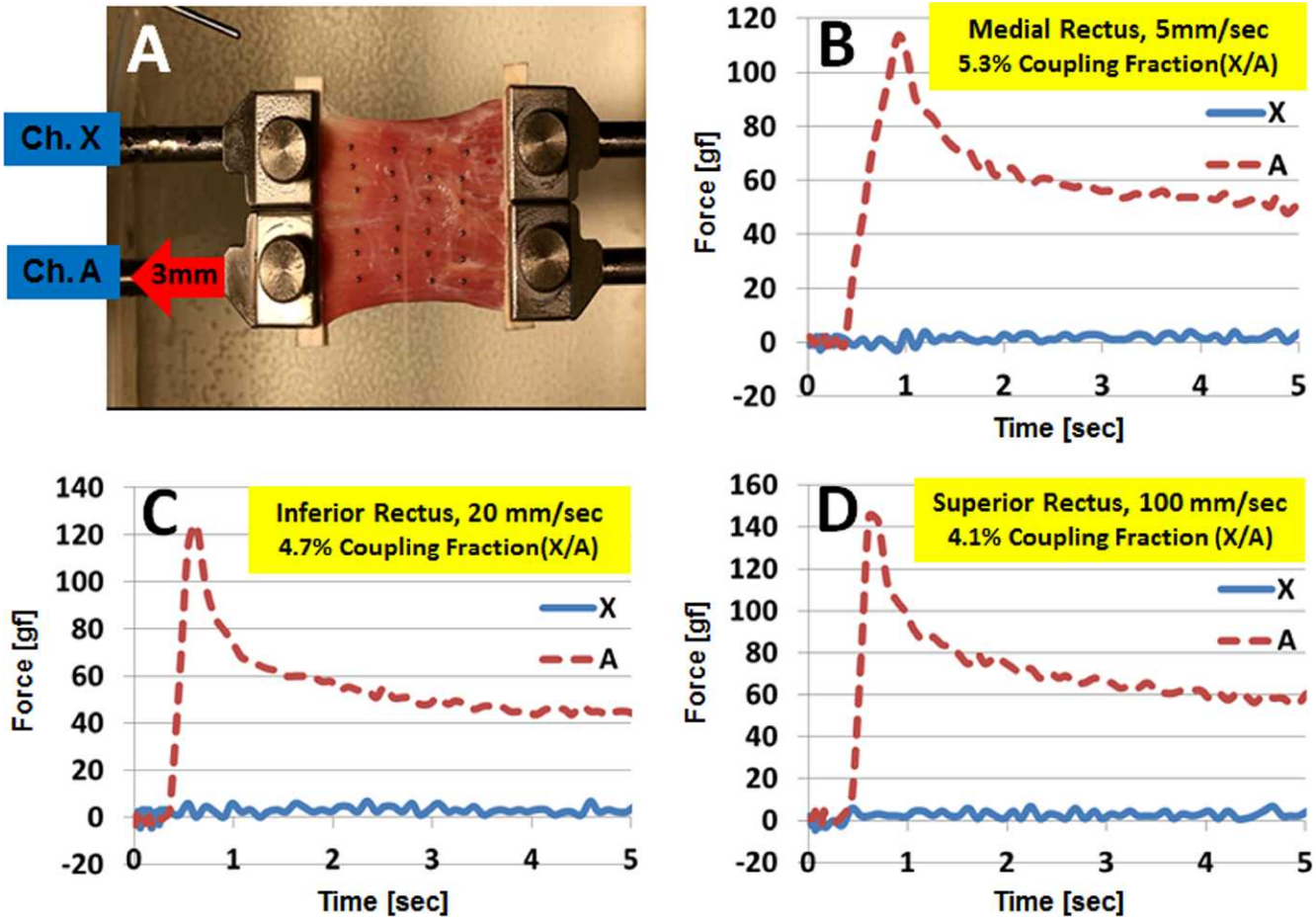

Figure 4. Examples of transverse compartment testing of three rectus EOMs. (**A**) Top-down view of one rectus EOM specimen with metal bead fiducials lying on the global surface. Specimen appears broad relative to its length because the terminal tendon was excised and because 5 mm at each end was incorporated within the clamps. *Channel A* was elongated to 3 mm to the left, while *channel X* was stationary. Graphs plot forces in each layer at 5 (*medial rectus*, [**B**]), 20 (*inferior rectus*, [**C**]), and 100 mm/sec (*superior rectus*, [**D**]) loading rates.

displacements in same column of fiducials were averaged, and compared along the EOM length for columns initially spaced 6 mm apart (Fig. 5). Since displacements in Figure 5 are cumulative displacements summed from the right to the left columns, local displacements can be calculated by subtraction between nearby column displacements. Local displacements for the moving compartment during five experiments averaged 792 ± 83 (SD), 522 ± 143, 521 ± 147, and 509 ± 87 μm, respectively, from first to fourth column. A similar computation was performed for the stationary compartment, resulting in 51 ± 98, 32 ± 64, 28 ± 34, and 14 ± 9 μm local displacements, respectively. The high SD values for the stationary compartment are caused by the shear force transfer described in the next paragraph. For both compartments, local displacement increased with distance from the fixed (origin) to the elongated specimen end (insertional tendon); of course as a boundary condition, there could have been no displacement at the fixed end clamp. The DRs from the first to fourth column were 5.4 ± 0.1%, 4.8 ± 0.1%, 4.2 ± 0.1%, and 2.9 ± 0.1%, respectively, indicating that the DR decreased from tendon end to origin.

In the displacement field for the stationary compartment, the fiducials mainly moved in the row closest to the boundary between compartments. Displacements of each row in the first column were 43 ± 11, 99 ± 12, and 235 ± 19 μm from top to bottom, respectively. This variation reflected shear force transfer. When the moving compartment elongated, shear force was generated at the boundary with the stationary compartment that is represented by the bottom row of fiducials. Since shear force declined with distance from the boundary, displacement declined accordingly.

Table 1. Transverse Compartment Coupling in EOMs at Three Loading Rates

	5 mm/s	20 mm/s	100 mm/s
Coupling fraction	5.6 ± 0.3%	4.9 ± 0.1%	4.1 ± 0.1%
F_s / F_m	6.3 gf / 111.9 gf	6.5 gf / 133.1 gf	5.8 gf / 142.4 gf
Displacement ratio	5.4 ± 0.1%	5.4 ± 0.1%	5.3 ± 0.1%

Five specimens were tested at each loading rate (mean ± SD). F_s is maximum force in stationary compartment. F_m is maximum force in moving compartment.

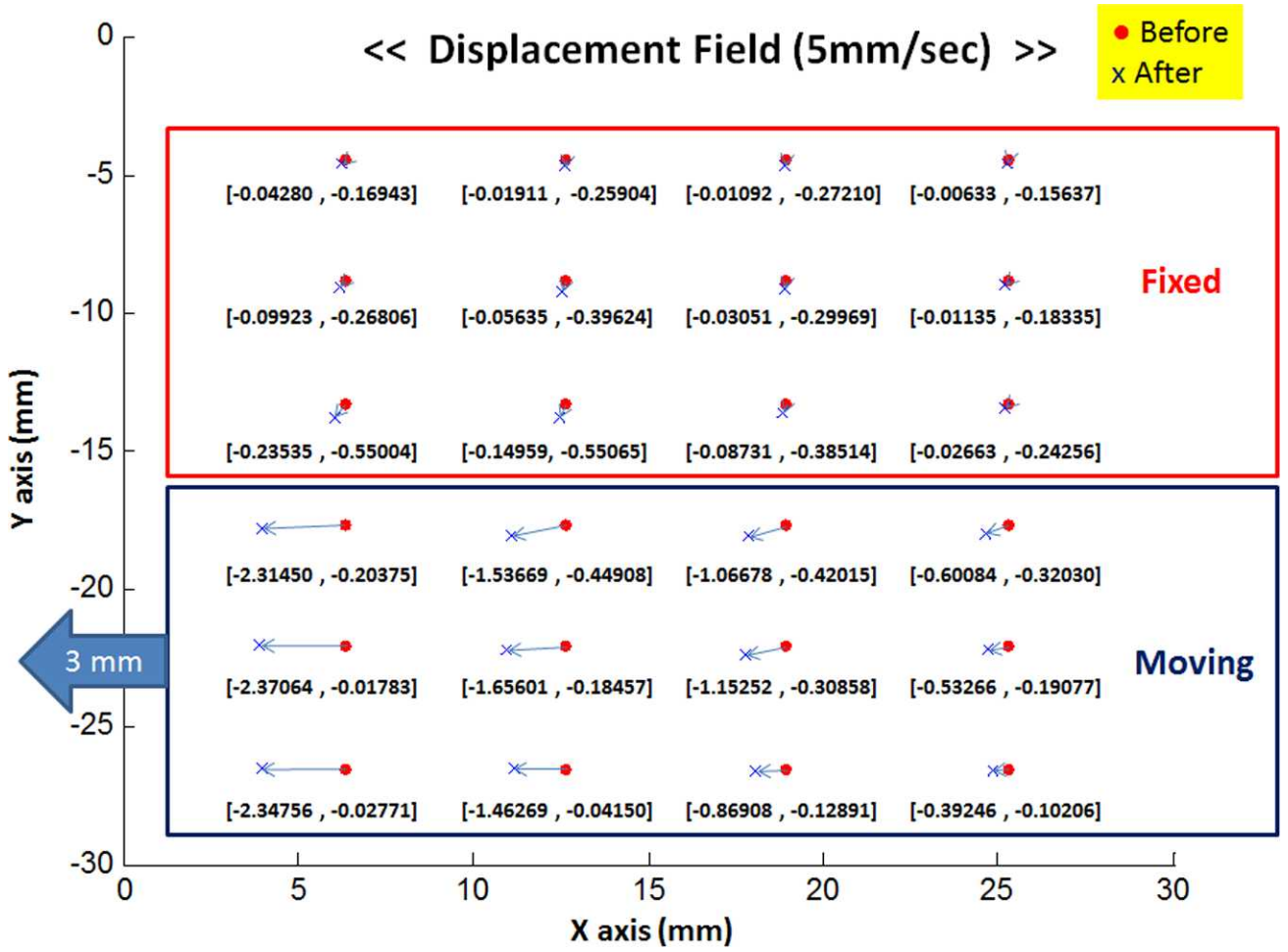

Figure 5. Displacement field of 6 × 3 mm fiducial array for tensile elongations of bovine EOMs at 5 mm/s. Five displacement results were averaged and visualized on the x-y plane.

Transverse Compartment Coupling in Six EOMs

Yoo et al.[37] have reported that the viscoelastic characteristics of all six bovine anatomical EOMs are similar, so it was of interest to compare compartmental coupling behavior among the anatomical EOMs. Three specimens of each anatomical EOM were subjected to 100-mm/sec tensile elongations using the foregoing experimental protocol. The observed CF values did not differ significantly among the six anatomical EOMs (Table 2, $P > 0.03$).

Coupling between Transverse Compartments of Unequal Proportions

Since the transverse proportion of horizontal rectus EOMs that is exclusively innervated by a single motor nerve division averages 50:50,[9] it was reasonable to have conducted the foregoing experiments with equal sized elongating and stationary compartments. However, since the anatomical proportions observed among individual EOM specimens range from 40:60 to 60:40, the mechanical effects of unequal sized compartments were investigated. Transverse compartment coupling experiments were performed in which the moving compartment constituted 60% (60:40 ratio) and 80% (80:20 ratio) of transverse EOM width. Four different EOM specimens were elongated at 100 mm/sec for each of the two ratios, yielding CF values of 3.7 ± 0.2%, and 3.0 ± 0.5%.

GL/OL Compartment Coupling

Experiments evaluating mechanical coupling between the GL and OL were performed similarly to experiments for the transverse compartments, except for use of orthogonal specimen clamping in the x-z plane. Since the OL and GL each exist across the entire transverse width of rectus EOMs, the width of the clamp was approximately double that for transverse compartment experiments, and forces generated were higher. Figure 6 illustrates GL/OL specimen placement and resulting force time series data. Twenty EOM specimens were tested at 5- and 100-mm/sec loading rates. For GL

Table 2. Mean (±SD) Tensile Force Coupling from Equal-Sized Elongating to Stationary Transverse Compartments of Each Anatomical EOM

Anatomical EOM	Lateral Rectus	Medial Rectus	Inferior Rectus	Superior Rectus	Inferior Oblique	Superior Oblique
Transverse coupling fraction	4.1 ± 0.1%	4.2 ± 0.1%	4.5 ± 0.2%	4.1 ± 0.1%	4.5 ± 0.3%	4.3 ± 0.2%

Three specimens each were tested at 100 mm/sec loading rate. None of the differences was statistically significant ($P > 0.03$).

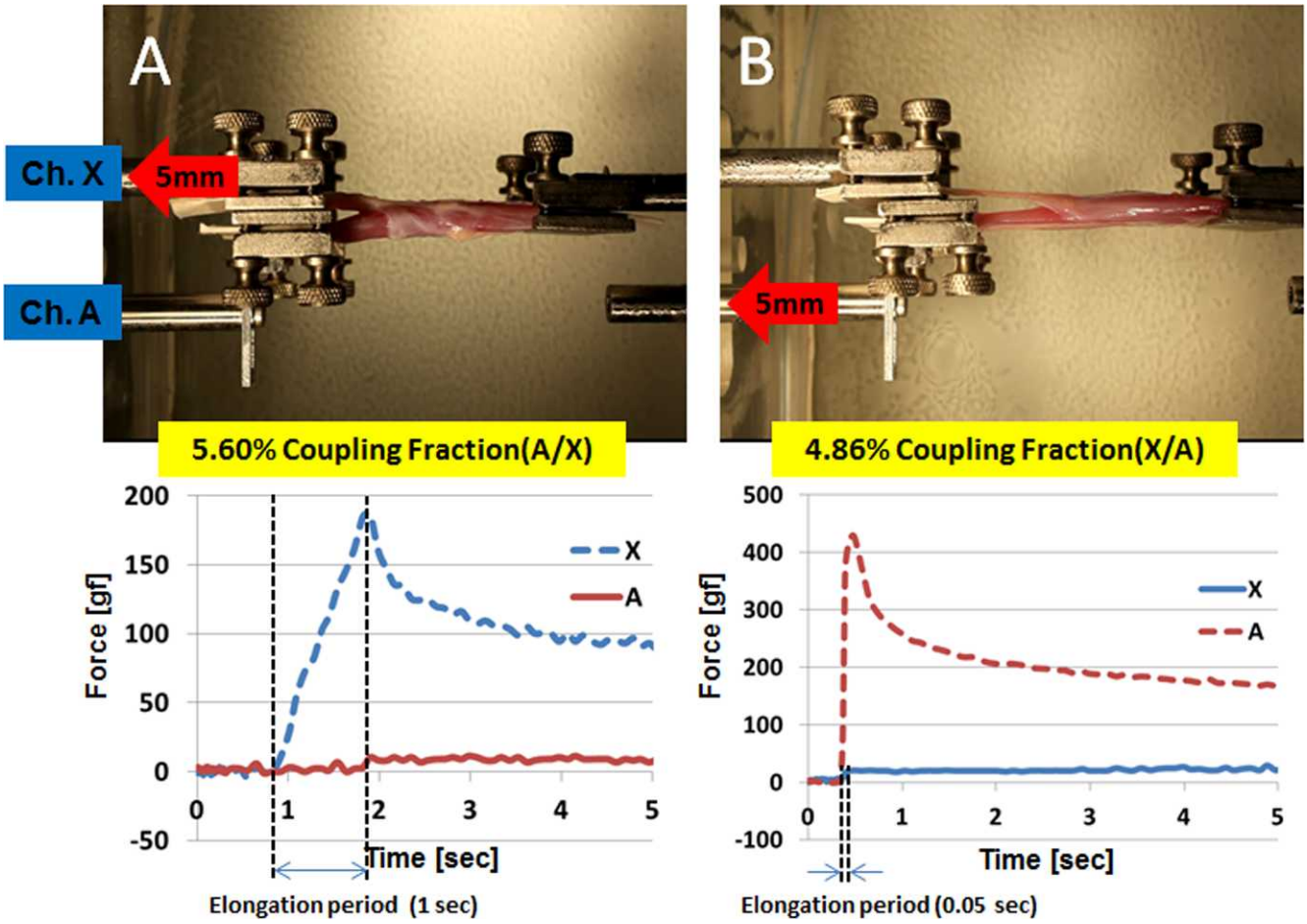

Figure 6. Examples of GL/OL compartment loading of two rectus EOMs. (**A**) OL extension in lateral rectus, 5 mm/sec (**B**) GL extension in medial rectus, 100 mm/sec.

elongations, mean CF values were 5.6 ± 0.4% and 4.9 ± 0.1%, respectively, while for OL elongations the mean CF values were 5.4 ± 0.4% and 4.5 ± 0.4% (Table 3). In each case, CF varied inversely to loading rate.

Tendon Compartment Coupling

Considering that all human rectus and the superior oblique EOMs insert on the globe via a tendon, mechanical coupling within tendon compartments was also investigated. For tendon compartment experiments, tendon from bovine horizontal rectus EOMs was sharply separated from the EOM bellies and subjected to the same experimental procedures as for transverse EOM compartments. Since tendon is stiffer than EOM, imposed elongations were smaller to avoid excessive tensile forces and specimen rupture. Five elongations of 0.2 or 0.3 mm at 5 mm/sec demonstrated an average CF of 3.3 ± 0.2%, a slightly lower CF than for EOM belly.

Table 3. Mean Coupling Fraction (±SD) between GL/OL Compartments during Tensile Loading

Rate	5 mm/s	100 mm/s
Coupling fraction		
OL loading	5.4 ± 0.4%	4.5 ± 0.4%
GL loading	5.6 ± 0.4%	4.9 ± 0.1%

Five specimens were tested at each loading rate.

Rubber Control Experiments

Since EOM is a highly orthotropic and flexible material, an isotropic and elastic rubber material (latex) was chosen as a control for the CF experiments. It was anticipated that the behavior of latex would differ substantially from that of EOM or tendon, because it was hypothesized that the independent mechanical behavior of the biological materials is related to their inhomogeneous internal structure. Samples with dimensions of 40×40×1.5 mm were prepared, with 1-mm elongation applied in the moving channel. The remaining experimental procedures were identical to those for EOM specimens. For rubber, mean CF values were 62.6 ± 1.6%, 55.0 ± 0.7%, and 50.0 ± 2.1%, respectively, at loading rates of 5, 20, and 100 mm/sec. As loading rate increased, CF decreased, consistent with the findings from EOM transverse compartmental loading experiments.

Orthogonal Loading Control Experiments

It was hypothesized that independence between longitudinal transverse and OL/GL compartments is due to anisotropic orientation of EOM and tendon fibers whose long directions parallel the long axis of each of these tissues, with relatively little coupling due to connective tissues or fiber-to-fiber junctions between the roughly parallel fibers. Physiologic loading is considered parallel to the lengths of the fibers. If that interpretation were true, it was predicted that repetition of the CF experiments after 90° reorientation of the specimens to

obtain nonphysiologic transverse loading would yield appreciably higher CF values than observed in the main experiment that employed longitudinal loading. Five specimens from lateral and inferior rectus EOMs were placed in the load cell so that their entire transverse widths, including both OL and GL, were incorporated into the adjacent fixed and moving sets of clamps. Since whole length of each EOM exceeds that of the clamp, excess EOM length was sharply excised. In each case, the posterior EOM was elongated by 3-mm orthogonal to the EOM's long axis, while force was recorded for the same direction in the stationary anterior EOM portion. The average orthogonal CF was 18.0 ± 3.4% (range 12.0%–21.0%), significantly greater than recorded under any condition during physiologic longitudinal elongation in the transverse compartment or OL/GL compartment experiments ($P < 0.002$).

Effect of Perimuscular Connective Tissues

To determine if removal of even the scant perimuscular connective tissues influences CF between compartments, control experiments were performed using specimens with all enveloping connective tissues intact. Five different specimens were clamped without removal of connective tissues, and subjected to procedures otherwise identical to the original transverse compartment experiments. Average CF was 5.9 ± 0.6%, which is similar to the result after removal of opaque enveloping connective tissue sheaths ($P > 0.3$), and confirming that the removal of this tissue did not influence the experimental results.

Compressive Loading Control Experiments

The mean CF of five specimens subjected to relative compressive loading was 5.5 ± 0.3%, similar to the results from tensile elongation ($P > 0.6$).

Discussion

These biomechanical experiments have demonstrated that adjacent but arbitrarily selected portions of EOMs and their tendons have a substantial degree of mechanical independence during longitudinal loading: less than 10% (typically much less) of the longitudinal tension in any one compartment was transmitted to the complimentary compartment, whether during extension or relative compression. This independence of tensile force in the physiologically generated, longitudinal direction was demonstrated between the OL and GL, as well as between transverse compartments of whole EOM and tendon ranging in ratio from 20:80, to 40:60, to 50:50 of transverse width. Compartmental independence was similar for all six anatomical EOMs. However, the same load cell apparatus demonstrated that this compartmentally independent, longitudinal mechanical behavior was quite different from the highly dependent behavior of an isotropic control material, latex rubber, implying that compartmental independence reflects the anisotropic structural properties of EOM and tendon. Further evidence that compartmental independence is related to tissue anisotropy is the finding that nonphysiologic, transverse loading of EOMs was associated with significantly less mechanical independence of adjacent regions.

Independence of longitudinal tensile force in transverse parsings of EOMs remained substantial and similar regardless of whether the transverse width of each EOM was arbitrarily divided into 50:50, 60:40, or 80:20 proportions. This suggests that any arbitrary groups of EOM fibers enjoy substantial mechanical independence from adjacent groups of fibers comprising the remainder of the EOM. It further implies that there is nothing special about mechanical intercoupling within adjacent groups of fibers that are mechanically tested together. While this biomechanical behavior was observed in all six anatomical EOMs, the biomechanical behavior only constitutes a condition necessary, but not itself sufficient, to permit physiologically independent compartmental function within an EOM. However, given the observed mechanical independence of these transverse grouping of EOM fibers, they could be coordinated into physiologically integrated compartments by appropriate local innervation whose distribution is limited only to the transverse extent of each compartment. Such compartmental segregation of intramuscular innervation has been demonstrated for the horizontal rectus EOMs of humans, monkeys, and other mammals,[8,9] but not in the vertical rectus EOMs. In other words, intramuscular motor nerve arborizations in the horizontal rectus EOMs do not cross transverse compartmental boundaries anywhere along the lengths of these EOMs, so the groups of EOM fibers separately innervated by the superior and inferior motor nerve trunks can constitute functionally independent superior and inferior muscle actuators whose tensions are delivered to separate insertions on the ocular sclera. Moreover, MRI has provided in vivo evidence of selective contraction in the superior versus inferior compartments of the human LR muscle during ocular counter-rolling, but not in the vertical rectus EOMs where intramuscular innervation is nonselective for compartments.[10,38] There is also MRI evidence that selective compartmental function in the medial rectus and to a lesser extent the lateral rectus may contribute to vertical duction in humans.[39] The markedly different electromyographic activity in the OL versus the GL of the human medial rectus is consistent with different function in these two layers.[40]

It is not unphysiologic, but indeed typical, for EOMs to undergo passive stretching by their antagonists. Although in the present study the EOMs did not generate active force by contracting, this study aimed to study mechanical force coupling between compartments. It was confirmed by control experiments that the intercompartmental coupling in EOM was similar for both elongation and shortening. Since both tensile and contractile tests demonstrate similar results for the CF, observed CF values appear relevant to EOM force transfer transverse to the directions of active sarcomere action. The findings are indisputably relevant to the behavior of EOM tendon.

It is notable that EOM compartments exhibit greater mechanical independence at higher, rather than lower, elongation velocities. As shown in Table 1, the relative intercompartmental coupling decreased as loading rate increased, while local strain, indicated by the displacement ratio, remained constant. This is primarily because maximum force in the moving compartment (F_m) increased with velocity due to viscous effects, while maximum displacement (D_m) was not altered by the loading speed. From Hook's law describing linear spring behavior, elastic force is proportional to displacement within the elastic limit. Consequently, EOM stiffness increased as loading rate increased, as is typical of any viscoelastic material. In addition, since there was minimal displacement in the fixed compartment, viscous effects were minimal there, so force changed little with loading rate. These findings further indicate that intercompartmental coupling is not appreciably mediated by viscous effects. Overall, this implies that compartmental independence between OL and GL is greater for fast eye movements such as saccades, than for steady fixations or slow movements such as pursuit. Furthermore, the current experiments demonstrated that portions of EOM tendon also exhibit substantial mechanical independence, permitting independent compartmental EOM contractile force to be transmitted independently to the globe.

Independence of tensile forces in EOM compartments was confirmed by observation of local displacement fields, for which there was also only approximately 5% coupling from the elongated to the stationary compartments. Modest variation in GL displacement fields along EOM lengths was probably caused by variation in EOM thickness. Since fusiform shaped, whole EOM was used for experiments, EOM thickness from anterior (tendon end) to posterior (origin end) increased. Therefore, local displacements tended to be large in the thinner part, and smaller in the thick part. The displacement fields also showed shift transverse to the elongation. This may have reflected both the mechanical coupling between longitudinal and transverse strain inherent in any material, as recognized in the classic Poisson ratio, but may also have reflected a contribution from EOM anatomy. In addition to connective within the EOM, tissue sheaths envelope the outside of each EOM so as to couple the two compartments transversely. When the moving compartment was elongated, it also underwent transverse strain that was partially coupled to the stationary compartment via the particular configuration of the transverse connective tissue sheaths. This effect was probably small, but would exaggerate the apparent CF, such that EOM compartments are probably more independent longitudinally than CF measurements would indicate.

At least some degree of mechanical independence between OL and GL is required by the APH, which postulates that the OL translates pulley connective tissues to influence EOM pulling direction, and the GL generates oculorotary tension to rotate the globe in the corresponding direction.[12–15] The present findings fulfill requirements of the APH, and consistent with observations of marked structural, electrophysiologic, hemodynamic, metabolic, and gene expression differences between OL and GL.[11–15]

The roughly parallel structure of EOM and tendon fibers probably is the dominant reason for the mechanical independence in compartments of EOM. Within EOM, fibers are arranged into fascicles of long, roughly parallel fibers. Anatomical studies have not been unanimous concerning the relative lengths of the fibers, or the configuration of their interconnections. In human and monkey, these fascicles extend most of the length of each rectus EOM, and exhibit few fiber-to-fiber junctions or fiber bifurcations when examined in serial sections stained by Masson trichrome.[17,18] While there have been reports of more myomyous junctions in such as cat,[19] rabbit,[21] and squirrel monkey,[41] their biomechanical importance has not been demonstrated directly, and may be consistent with the low CF observed in the current study. Even if some anatomical couplings do occur among EOM fibers, the well known compartmental specialization of numerous skeletal muscles demonstrates that partial couplings do not preclude substantially independent physiological actions. For example, gastrocnemius,[1] trapezius,[2] transversus abdominis,[3] cricothyroid,[4] and triceps brachii muscles[5] are comprised of multiple neuromuscular compartments that are controlled by independent motor neuron pools. The much higher CF observed for transverse as compared with longitudinal EOM elongations clearly demonstrate that fiber orientation plays a major role in force coupling among adjacent EOM regions.

The current findings of substantial mechanical independence of adjacent portions of EOM tendon have clinical correlated. Tenotomy of only a portion of the fibers in vertical rectus EOM tendons has long been practiced for the treatment of small angle vertical strabismus,[42–45] and more recently of the horizontal rectus tendons for treatment of A and V pattern horizontal strabismus.[46] The present biomechanical findings permit the inference that surgical division from the scleral insertion of a portion of the fibers of a rectus tendon would release the tension in those fibers, while maintaining nearly unchanged the tension in the fibers that remain attached to the sclera. This interpretation is consistent with the finding of a predictable relationship between the percentage of vertical rectus tenotomy and the degree of correction of vertical strabismus in humans.[47] Selective regional surgery on the broad superior oblique (SO) tendon has long been practiced to selectively manipulate the vertical actions effected by the posterior tendon fibers, versus torsional actions effected by the anterior fibers.[48–53]

Taken together, the current findings indicate that EOM and tendon have sufficient biomechanical independence to support the proposed functional diversity of actions in distinct neuromuscular compartments of the horizontal rectus EOMs, and following regionally selective surgical manipulations in rectus and oblique extraocular tendon. Since biomechanical independence only affords the opportunity, and not the obligation, of physiologic independence of groups of fibers within any given EOM, it remains to be determined the extent to which innervational control coordinates or distinguishes the contractile activity of EOM subparts during the physiologic and pathologic ocular motor repertoire.

Acknowledgments

The authors thank Manning Beef, LLC, Pico Rivera, CA, for their generous contribution of bovine specimens, and Jose Martinez, Claudia Tamayo, and Ramiro Carlos for assistance with specimen preparation.

References

1. English AW, Wolf SL, Segal RL. Compartmentalization of muscles and their motor nuclei: the partitioning hypothesis. *Phys Ther*. 1993;73:857–867.
2. Holtermann A, Roeleveld K, Mork PJ, et al. Selective activation of neuromuscular compartments within the human trapezius muscle. *J Electromyogr Kinesiol*. 2009;19:896–902.
3. Urquhart DM, Hodges PW. Differential activity of regions of transversus abdominis during trunk rotation. *Eur Spine*. 2005; 14:393–400.
4. Mu L, Sanders I. The human cricothyroid muscle: three muscle bellies and their innervation patterns. *J Voice*. 2009;23:21–28.
5. Lucas-Osma AM, Collazos-Castro JE. Compartmentalization in the triceps brachii motoneuron nucleus and its relation to muscle architecture. *J Comp Neurol*. 2009;516:226–239.
6. Goldberg SJ, Wilson KE, Shall MS. Summation of extraocular motor unit tensions in the lateral rectus muscle of the cat. *Muscle Nerve*. 1997;20:1229–1235.
7. Goldberg SJ, Meredith MA, Shall MS. Extraocular motor unit and whole-muscle responses in the lateral rectus muscle of the squirrel monkey. *J Neurosci*. 1998;18:10629–10639.
8. Peng M, Poukens V, da Silva Costa RM, Yoo L, Tychsen L, Demer JL. Compartmentalized innervation of primate lateral rectus muscle. *Invest Ophthalmol Vis Sci*. 2010;51:4612–4617.
9. da Silva Costa RM, Kung J, Poukens V, Yoo L, Tychsen L, Demer JL. Intramuscular innervation of primate extraocular muscles: unique compartmentalization in horizontal recti. *Invest Ophthalmol Vis Sci*. 2011;52:2830–2836.
10. Clark RA, Demer JL. Differential lateral rectus compartmental contraction during ocular counter-rolling. *Invest Ophthalmol Vis Sci*. 2012;53:2887–2896.
11. Demer JL, Oh SY, Poukens V. Evidence for active control of rectus extraocular muscle pulleys. *Invest Ophthalmol Vis Sci*. 2000;41:1280–1290.
12. Demer JL. The orbital pulley system: a revolution in concepts of orbital anatomy. *Ann N Y Acad Sci*. 2002;956:17–32.

13. Demer JL. Pivotal role of orbital connective tissues in binocular alignment and strabismus. The Friedenwald lecture. *Invest Ophthalmol Vis Sci*. 2004;45:729–738.
14. Demer JL. Current concepts of mechanical and neural factors in ocular motility. *Curr Opin Neurol*. 2006;19:4–13.
15. Demer JL. Mechanics of the orbita. *Dev Ophthalmol*. 2007;40: 132–157.
16. Martini FH, Timmons MJ, Tallitsch RB. *Human Anatomy (6th Edition)*. San Francisco: Benjamin Cummings; 2008.
17. Lim KH, Poukens V, Demer JL. Fascicular specialization in human and monkey rectus muscles: Evidence for anatomic independence of global and orbital layers. *Invest Ophthalmol Vis Sci*. 2007;48:3089–3097.
18. Demer JL, Poukens V, Ying H, Shan X, Tian J, Zee DS. Effects of intracranial trochlear neurectomy on the structure of the primate superior oblique muscle. *Invest Ophthalmol Vis Sci*. 2010;51:3485–3493.
19. Mayr R, Gottschall J, Gruber H, Neuhuber W. Internal structure of cat extraocular muscle. *Anat Embryol*. 1975;148:25–34.
20. Davidowitz J, Philips G, Breinin GM. Organization of the orbital surface layer in rabbit superior rectus. *Invest Ophthalmol Vis Sci*. 1977;16:711–729.
21. McLoon LK, Rios L, Wirtschafter JD. Complex three-dimensional patterns of myosin isoform expression: differences between and within specific extraocular muscles. *J Muscle Res Cell Motil*. 1999;20:771–783.
22. Harrison AR, Anderson BC, Thompson LV, McLoon LK. Myofiber length and three-dimensional localization of NMJs in normal and botulinum toxin–treated adult extraocular muscles. *Invest Ophthalmol Vis Sci*. 2007;48:3594–3601.
23. Tsai SW, Hahn HT. *Introduction to composite materials. Lancaster: Technomic Publishing Company*; 1980.
24. Lekhnitskii SG. *Theory of elasticity of an anisotropic elastic body. San Francisco: Holden-Day*; 1963.
25. Vasiliev VV. *Mechanics and analysis of composite materials*. New York: Elsevier; 2001.
26. Liu JY. Effects of shear coupling on shear properties of wood. *Wood Fiber Sci*. 2000;32:458–465.
27. Whitney JM. Elastic moduli of unidirectional composites with anisotropic filaments. *J Compos Mater*. 1967;1:188–193.
28. Broutman LJ. Measurement of the fiber-polymer matrix interfacial strength. *Interfaces in Composites, ASTM STP 452*. 1969;27–41.
29. Takaku A, Arridge RC. The effect of interfacial radial and shear stress on fibre pull-out in composite materials. *J Phys D Appl Phys*. 1973;6:2038–2047.
30. Gray RJ. Analysis of the effect of embedded fibre length on fibre debonding and pull-out from an elastic matrix. *J Mater Sci*. 1984;19:861–870.
31. Kelly A, Tyson WR. Tensile properties of fibre-reinforced metals: copper/tungsten and copper/molybdenum. *J Mech Phys Solids*. 1965;13:329–350.
32. Cox HL. The elasticity and strength of paper and other fibrous materials. *Brit J Appl Phys*. 1952;3:72–79.
33. Amirbayat J, Hearle JWS. Properties of unit composites as determined by the properties of the interface. Part I: mechanism of matrix-fibre load transfer. *Fibre Sci Technol*. 1969;2:123–141.
34. Mandell JF, Chen J-H, McGarry FJ. A microdebonding test for in-situ fiber-matrix bond and moisture effects. *Research Report R80-1*. Cambridge, MA: Dept Mater Sci & Eng, MIT. 1980.
35. Grande DH, Mandell JF, Hong KCC. Fibre-matrix bond strength studies of glass, ceramic, and metal matrix composites. *J Mater Sci*. 1988;23:311–328.
36. Netravali AN, Stone D, Ruoff S, Topoleski LTT. Continuous micro-indenter push-through technique for measuring interfacial shear strength of fiber composites. *Compos Sci Technol*. 1989;34:289–303.
37. Yoo L, Kim H, Gupta V, Demer JL. Quasilinear viscoelastic behavior of bovine extraocular muscle tissue. *Invest Ophthalmol Vis Sci*. 2009;50:3721–3728.
38. Demer JL, Clark RA, da Silva Costa RM, Kung J, Yoo L. Expanding repertoire in the oculomotor periphery: selective compartmental function in rectus extraocular muscles. *Ann N Y Acad Sci*. 2011;1233:8–16.
39. Clark RA, Demer JL. Functional morphometry of horizontal rectus extraocular muscles during horizontal ocular duction. *Invest Ophthalmol Vis Sci*. 2012;53:7375–7379.
40. Collins CC. The human oculomotor control system. In: Lennerstrand G, Bach-y-Rita. P, eds. *Basic Mechanisms of Ocular Motility and Their Clinical Implications*. Oxford, New York: Pergamon Press; 1975:145–180.
41. Shall MS, Dimitrova DM, Goldberg SJ. Extraocular motor unit and whole-muscle contractile properties in the squirrel monkey. *Exp Brain Res*. 2003;151:338–345.
42. Wright KW. Mini-tenotomy procedure to correct diplopia associated with small-angle strabismus. *Trans Am Ophthalmol Soc*. 2009;107:97–102.
43. Yim HB, Biglan AW, Cronin TH. Graded partial tenotomy of vertical rectus muscles for treatment of hypertropia. *Trans Am Ophthalmol Soc*. 2004;102:169–175. discussion 175–166.
44. Von GA. Beitrage zur Lehre vorn Schielen und den Schiel Operationen. *Arch Ophtalmol*. 1857;3:177–386.
45. Howe L. Partial tenotomy. In: Howe L, ed. *The Muscles of the Eye*. London, New York: GP Putnam's Sons/The Knickerbocker Press; 1908:304–308.
46. van der Meulen-Schot HM, van der Meulen SB, Simonsz HJ. Caudal or cranial partial tenotomy of the horizontal rectus muscles in A and V pattern strabismus. *Br J Ophthalmol*. 2008;92:245–251.
47. Chaudhuri A, Hendler K, Demer JL. Graded rectus tenotomy in small angle hypertropia due to sagging eye syndrome. *Absrt Ann Mtg of Am Assoc Ped Ophthalmol Strabismus*. In press.
48. Vempali VMR, Lee JP. Results of superior oblique posterior tenotomy. *J AAPOS*. 1998;2:147–150.
49. Gobin M. Posterior tenotomy of the superior oblique muscle in A-pattern squint [in French]. *Bull Soc Belge Ophtalmol*. 1978;182:104–113.
50. Graf M, Krzizok T, Kaufmann H. Combined oblique muscle operation with transposition of the insertion in strabismus sursoadductorius [in German]. *Klin Monbl Augenheilkd*. 1994;205:329–335.
51. Souza-Dias C, Uesugui C. Efficacy of different techniques of superior oblique weakening in the correction of the "A" anisotropia. *J Pediatr Ophthalmol Strabismus*. 1986;23:82–86.
52. Yagasaki T, Nomura H, Koura T, Sato M, Awaya S. Posterior tenotomy of the superior oblique at the scleral insertion for A-pattern deviations. *Jpn J Ophthalmol*. 1995;39:83–88.
53. Kushner BJ. Effect of ocular torsion on a and v patterns and apparent oblique muscle overaction. *Arch Ophthalmol*. 2010; 128:712–718.